

# Circuit Agility

*Errikos Lourandakis, Robert Weigel,  
Henning Mextorf, and Reinhard Knoechel*

Over the last decade, mobile communication and its associated mass volume market has become one of the driving forces in the technology evolution of semiconductor and microwave circuits. For handheld communication devices, it is now mainstream to support increasing numbers of communication standards and localization services that

occupy ever-expanding wide frequency ranges and bandwidths. At the same time, the physical dimensions of handheld user devices are shrinking, leading to even tighter specifications for the highly integrated front-end architectures of mobile radios. Today's radio front-end architectures use dedicated receive and transmit paths for each covered communication standard, thus the overall complexity and occupied area

---

*Errikos Lourandakis (e.lourandakis@helic.com) is with Helic S.A., Sorou 12, GR15125 Athens, Greece. Robert Weigel is with the Institute for Electronics Engineering, University of Erlangen-Nuremberg, Cauerstrasse 9, 91058 Erlangen, Germany. Henning Mextorf and Reinhard Knoechel are with the Institute of Electrical and Information Engineering, Microwave Research Laboratory University of Kiel, Kaiserstrasse 2, 24143 Kiel, Germany.*

Digital Object Identifier 10.1109/MMM.2011.2173987

Date of publication: 13 January 2012

## Over the last decade, mobile communication and its associated mass volume market has become one of the driving forces in the technology evolution of semiconductor and microwave circuits.

is increasing as well. The wide frequency allocation of the regulated communication bands along with the variety of standards, which have to be covered by these radios, calls for reconfigurable and frequency agile microwave subsystems. By introducing such subsystems, new architectures with reduced numbers of functional blocks could be implemented. The scope of this article is to provide a comprehensive understanding of design principles for frequency agile and reconfigurable microwave circuits such as power dividers and couplers and how they can be used in radio-frequency (RF)-transceiver subsystems to pave the way toward reconfigurable radio front-end architectures. Introducing reconfigurability in microwave circuits is achieved by tunable passive components. Tunable passives can be implemented in a variety of technologies such as ferroelectric varactors, semiconductor diodes, and microelectromechanical systems (MEMS) components. Attractive applications for tunable circuits in the RF front end are tunable matching networks [1], [2], filters [3], [4], reconfigurable power amplifiers [5], [6], tunable voltage controlled oscillator (VCO) circuits [7], and, finally, couplers and dividers.

### Coupler Theory

Microwave power dividers and couplers have been used in various applications such as Doherty amplifiers [31] and balanced amplifiers [32]. Tight coupling structures, such as 3 dB couplers, are not easily implemented with planar-coupled lines due to very narrow spacing between the line segments that are difficult to fabricate. Other topologies such as Wilkinson power dividers and branch-line couplers are therefore usually considered for these applications. Such circuits also serve as building blocks for other topologies such as six-port receivers used for localization

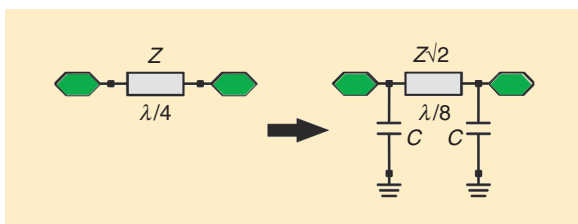


**Figure 1.** Quarter-wavelength segment and its equivalent lowpass circuit.

[8] or communication applications [9]. Modified coupler topologies have been reported using defected ground structures [10], and dual band operation for couplers is achieved by multiple resonator branches [11] or left-handed transmission lines [12]. Systematic design methodologies for frequency agile and reconfigurable microwave couplers will be presented in the following sections. Reconfigurable characteristics are achieved by introducing tunable passive components such as ferroelectric varactors or semiconductor diodes. In the following section a discussion of coupler theory is introduced to give the reader a background into some of the challenges involved in the design of these circuits.

### Frequency Agile Couplers

A closer look at widely used coupler/divider topologies such as the Wilkinson power divider and branch-line coupler reveals that the fundamental building blocks are quarter-wavelength transmission line segments at the design frequency. The proposed reconfigurable coupler design methodology is based on the principle of substituting  $\lambda/4$  segments with equivalent lowpass structures [13]. The resulting new transmission line segments are made significantly shorter by raising their characteristic impedance and adding shunt capacitors at the ends, as indicated in Figure 1.

The capacitance value for the equivalent lowpass structure can be calculated by comparing the network parameter matrix of the quarter-wavelength segment with the corresponding matrix of the lowpass structure [14]. By calculation, it is easily seen that the shunt capacitance is described by a closed form solution of the following form

$$C = 1/(2\pi f Z \sqrt{2}). \quad (1)$$

By using the capacitances shown (1), it is possible to design fully scalable equivalent quarter-wavelength transmission line segments. For each starting characteristic impedance  $Z$  and resonance frequency  $f$ , a single capacitance value  $C$  can be calculated and, by changing the capacitance value  $C$  (for example by using a varactor), the resonance frequency  $f$  is altered. Limiting factors to this approach arise due to the resulting impedance values for real implementations using microstrip or coplanar waveguide technology. The same approach can be applied to lumped element inductance and capacitance (LC) equivalent lowpass circuits in lieu of transmission line sections [15]. By understanding this operational principle, designs of more complex topologies that are based on  $\lambda/4$  transmission line segments can be implemented. An alternative approach of achieving frequency agile behavior for a symmetrical four-port network is considered in [16] and is based on the manipulation of the network eigen-reflection parameters (see "Definitions").

## Definitions

### Eigenreflections

Eigenreflections are the eigenvalues of the scattering matrix of a symmetrical network. The scattering parameters can be calculated from these eigenvalues and the corresponding eigenvectors. This is crucial because the eigenvalues and eigenvectors usually can be determined easily using an even-odd-mode analysis.

### Electric and Magnetic Wall

The electromagnetic conditions for electric and magnetic walls are that there are no tangential fields but only normal field components of the electric and the magnetic field, respectively, at the wall boundary. Those conditions are also referred to as "short circuit" and "open circuit."

## Wilkinson Divider

As opposed to other power-divider structures such as T-splitters or resistive dividers, the Wilkinson divider is matched at all ports while achieving perfect isolation between the outputs at the resonance frequency. The input and output port impedances are  $Z_0$  while the  $\lambda/4$  segments have a characteristic impedance of  $Z_0\sqrt{2}$ . The output ports 2 and 3 are connected through a resistor with  $R = 2Z_0$  thus enabling impedance matching at all ports and isolation between them. Symmetric power splitting is achieved with no phase difference ( $\Delta\phi = 0^\circ$ ) for the two transmission paths (ports 2 and 3).

Using the addition of a shunt capacitance as previously described, a reduced size topology of the original Wilkinson divider is presented in Figure 2(b). The new transmission line segments have a shorter electrical length and higher characteristic impedance. The  $\lambda/4$  transmission line segment of impedance  $Z_0\sqrt{2}$  can be substituted by an equivalent segment of length  $\lambda/8$  with an impedance of  $2Z_0$  by adding two lumped capacitors to the transmission line, with a capacitance value of  $C = 1/(4\pi f Z_0)$ .

A similar approach for the substitution of the quarter-wavelength segment is discussed in [25] and results in the lumped elements along with transmission lines forming an equivalent hybrid circuit. An input transformer implemented as a T-network combined with a second semilumped output loop, as shown in Figure 3, results in a tunable power divider.

By adjusting the capacitance  $C_1$ , the input impedance and the operating frequency of the divider is altered. The second capacitance  $C_2$  provides an additional degree of tuning freedom and is varied to achieve optimum isolation between the output ports of the divider at each operating frequency. The resulting total length of the

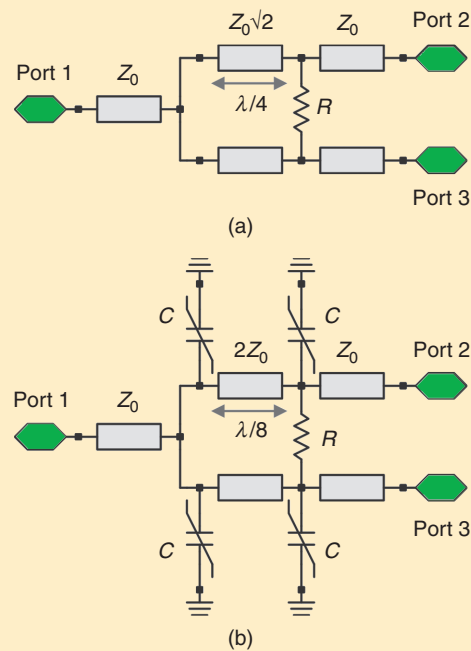


**Figure 2.** (a) Wilkinson divider and (b) reduced size frequency agile divider.

transmission line segments in this topology is approximately  $\lambda_1 + \lambda_2 + \lambda_3 \approx \lambda/8$ , thus achieving a size reduction comparable to the previously described equivalent lowpass approach. As it is the case for the equivalent circuit of Figure 2, the input transformer of the topology in Figure 3 exhibits a lowpass behavior achieving harmonic suppression at the output ports as well.

## Branch-Line Coupler

Quadrature hybrids, also called "branch-line couplers," are four-port couplers based on quarter-wavelength segments and have the structure shown in Figure 4. The input power at port 1 is equally divided at the output ports 2 and 3 at the  $\lambda/4$  resonance frequency with port 4 isolated. The output signals have a phase difference of  $\Delta\phi = 90^\circ$ . The characteristic impedance of the series branches is  $Z_0/\sqrt{2}$ , whereas the parallel branches have a characteristic impedance of  $Z_0$ .

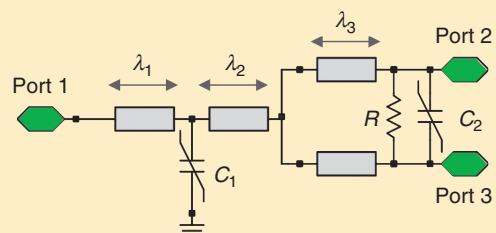


**Figure 3.** Schematic of tunable power divider using impedance transformer and output loop with electronically tunable capacitors.

## There are three general types of couplers: the forward coupler, the transverse coupler, and the backward coupler.

The reduced size topology in Figure 4(b) uses the same principle as the previously discussed power divider. The resonator segments between all ports have been scaled according to their initial characteristic impedance by using (1). For size and component count reasons, the individual capacitances at each corner of the coupler have been combined into a single

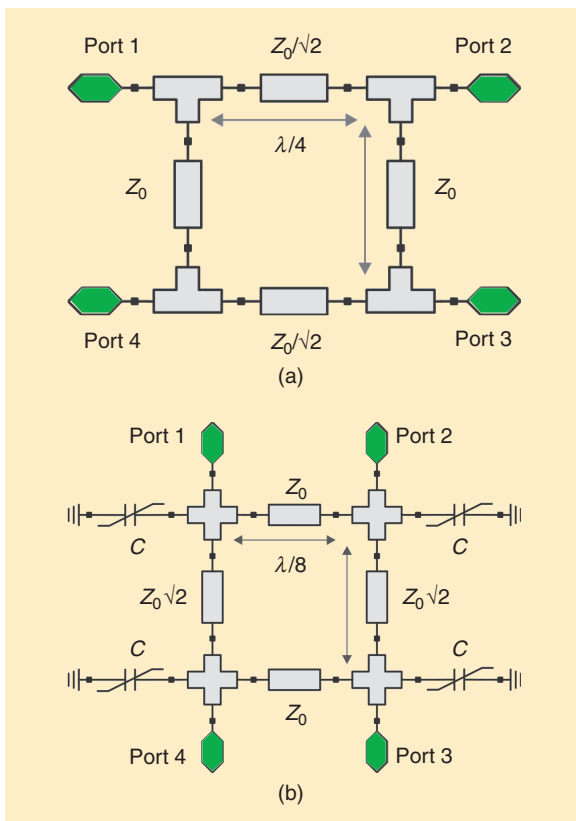


**Figure 4.** (a) Branch-Line coupler and (b) reduced size frequency agile coupler with electronically tunable capacitors.

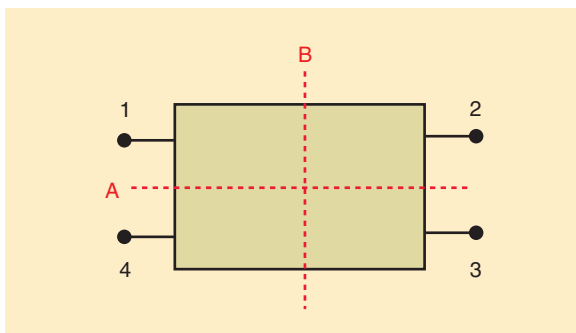


**Figure 5.** Two-fold symmetrical four-port.

capacitance with value  $C = (1 + \sqrt{2}) / (2\pi f Z_0 \sqrt{2})$ . As in the case of the power divider shown in Figure 2, the design is based on scalable equations that can be translated into the desired frequency and impedance range as long as the resulting impedance values can be fabricated in the desired technology.

### Quadrature Couplers

Microwave networks are commonly described in terms of wave quantities such as incident and reflected waves at each port. Voltage excitation at one port while the other ports are perfectly terminated, and vice versa, allows for a description of the wave quantities between all network ports. Scattering parameters are primarily used for defining the relations between these wave quantities. The scattering-parameters of the two-fold symmetrical four-port shown in Figure 5 with symmetry planes A and B can be determined by using an even-odd-mode analysis by the application of in-phase and out of phase signals (even-odd mode excitation) at each port and observing the resulting response at the other ports.

An extension of the method of Reed and Wheeler [17] with even and odd excitations in both symmetry planes leads to a decomposition of the four-port into a number of single-ports. Four one-ports terminated with different configurations of electric wall (ew) and magnetic wall (mw) occur as shown in Figure 6 (see “Definitions”).

The scattering-parameters are then linear combinations of the four eigenreflections [18]:

$$S_{11} = S_{22} = S_{33} = S_{44} = \frac{1}{4}(r_{ee} + r_{de} + r_{ed} + r_{dd}), \quad (2)$$

$$S_{21} = S_{12} = S_{43} = S_{34} = \frac{1}{4}(r_{ee} + r_{de} - r_{ed} - r_{dd}), \quad (3)$$

$$S_{31} = S_{13} = S_{42} = S_{24} = \frac{1}{4}(r_{ee} - r_{de} - r_{ed} + r_{dd}), \quad (4)$$

$$S_{41} = S_{14} = S_{32} = S_{23} = \frac{1}{4}(r_{ee} - r_{de} + r_{ed} - r_{dd}). \quad (5)$$

If the four-port with two-fold symmetry is considered lossless, the absolute values of the eigenreflections are one. In order to match the circuit, the positions of the eigenreflections in the complex plane have to be

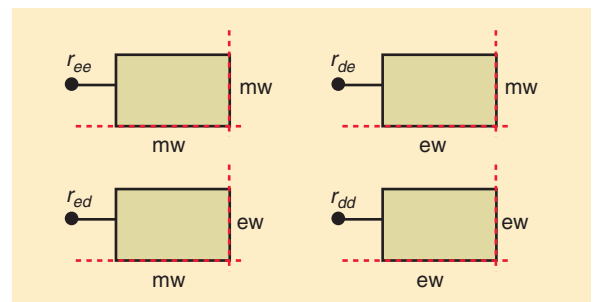


**Figure 6.** Equivalent one-ports with even- and odd-mode excitations.

chosen so that they form two antiparallel oriented pairs. If the three criteria (two-fold symmetry, lossless, and port-matching) are fulfilled, the four-port will be a quadrature directional coupler with one port decoupled and the phase difference between the two output ports 90°. There are three general types of couplers: the forward coupler, the transverse coupler, and the backward coupler. The type and the coupling level is dependent on the positions of the eigenreflections. A constellation example of the eigenreflections of a 3 dB forward coupler is given in Figure 7. The eigenreflection pairs  $r_{ee}$ ,  $r_{ed}$  and  $r_{de}$ ,  $r_{dd}$  are antiparallel, thus fulfilling the previously described requirements.

A quadrature directional coupler with variable coupling ratio can be realized by deliberately rotating the eigenreflections in the complex plane. Therefore, a potential two-fold symmetric coupler structure is analyzed using the even-odd analysis. Then it can be seen how the variation of circuit elements in the original structure affects the positions of the eigenreflections and if there is a need for additional tuning elements in order to fulfill the matching criterion. Ideally, the eigenreflections form two antiparallel pairs at any time to ensure perfect matching. The magnitude of the output scattering-parameters depends on the angle  $\alpha$  between the two pairs of antiparallel eigenreflections. This leads to a rule for the dependence of the tuning elements with respect to each other. Using this rule, a systematic design of couplers having continuously tunable coupling ratios is possible [16], [18].

An easier way to design directional couplers with continuously tunable coupling ratios is to cascade two quadrature directional couplers having either a tunable phase shifter in one connection branch [19], [20] or tunable discontinuities in both connection branches [21]–[23]. With this kind of approach, there is no modification of the original coupler structure and off-the-shelf couplers can be used. Tunable forward and backward couplers can be easily designed with this technique [24].

### Frequency Agile Microwave Circuits

The previous section provided the background for the systematic design of reconfigurable couplers and dividers using a lowpass structure with tunable capacitors. This design methodology is now applied to the development of a number of prototype circuits (Wilkinson divider and branch-line coupler) with measured data showing how well this design methodology works as well as some of the performance limitations of these reconfigurable coupler/dividers.

#### Wilkinson Divider

A prototype of a reduced-size frequency agile Wilkinson divider for use in the 2.0 GHz range was fabricated on a Rogers RO3010 substrate and is shown in Figure 8(a). Ideally, such a tunable power divider should cover the entire frequency range from 1.7–2.4 GHz, which is

**Ideally, the eigenreflections form two antiparallel pairs at any time to ensure perfect matching.**

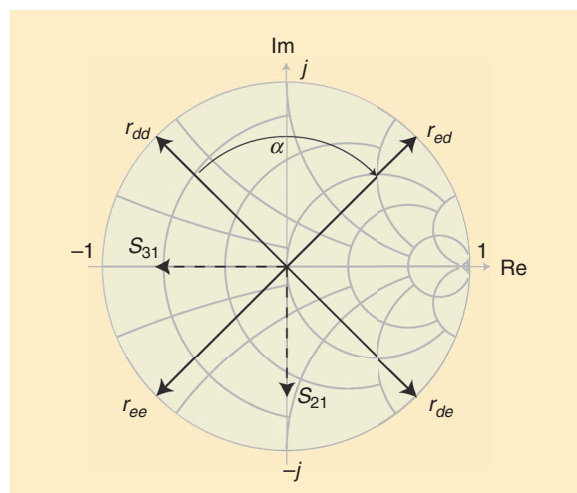


**Figure 7.** Smith chart constellation of the eigenreflections of a 3 dB forward coupler.

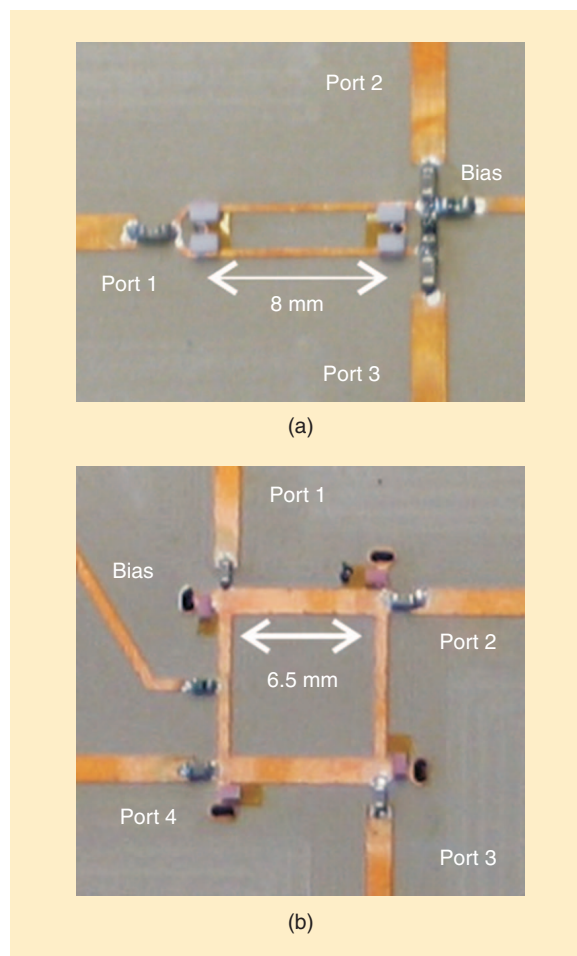


**Figure 8.** Fabricated prototype boards of frequency agile microwave circuits: (a) Wilkinson divider and (b) branch-line coupler.

currently used for mobile communications. Equal 3 dB power splitting and sufficient isolation is targeted at all operating frequencies. There are dc-block capacitors placed at all RF ports, and one RF choke inductor is employed to isolate the tuning voltage used to establish the proper bias conditions for the ferroelectric tuning varactors. Based on the previous analysis, for a system impedance of  $Z_0 = 50 \Omega$ , varactors with a nominal maximum capacitance of 1 pF were used. Varactor tunability, defined as  $(C_{\max} - C_{\min}) / C_{\max}$ , of approximately 60% is achieved for the used ferroelectric thin-film capacitors at bias voltages of 20 V. At frequencies around 2 GHz, the maximum quality factor  $Q$  of the varactors is about 30. Moderate  $Q$  factors also set the limitations in terms of operating frequency for these example circuits. All varactors were assembled in a flip-chip procedure in order to eliminate the resulting parasitic wire inductance and the associated loss mechanisms of conventional wire assemblies. Stud bumps were placed on the varactor dies, and a conductive adhesive ensured proper electrical contact with the printed circuit board (PCB).

Varactor tunability and the detuning of the characteristic impedance of the equivalent lowpass segments limit the divider tuning range from 1.7 GHz to

2.1 GHz, resulting in a tunability  $(f_{\max} - f_{\min}) / f_{\min}$  of 23% (Figure 9). The insertion loss of the circuit, compared to the ideal 3 dB power splitting, varies from 0.6 dB to 1.2 dB within the operating bandwidth of each state. Symmetrical power splitting is achieved in both amplitude and phase, thus fulfilling the divider operation. The worst case amplitude and phase difference is 0.5 dB and  $8^\circ$ , respectively. All figures reveal the inherent lowpass behavior, thus harmonic radiation would be suppressed significantly when considering an operation in a transceiver front-end system. At all operating bias states, the second harmonic is attenuated by more than 20 dB.

As a comparison with the Wilkinson divider described previously, a prototype implementation and experimental results of a tunable 2:1 power divider based on a ring structure from [25] is shown in Figure 10. The power divider is tuned from 0.9 GHz to 1.7 GHz by using varactor diodes as tuning elements, achieving a tunability of 89%. The broad tuning range for this divider is achieved by varactor diodes with a  $C_{\max} / C_{\min}$  of more than 5:1. Lowpass filtering is achieved at the divider outputs similar to the previously discussed power divider from [14]. Tuning independently, the two varactors used in this topology

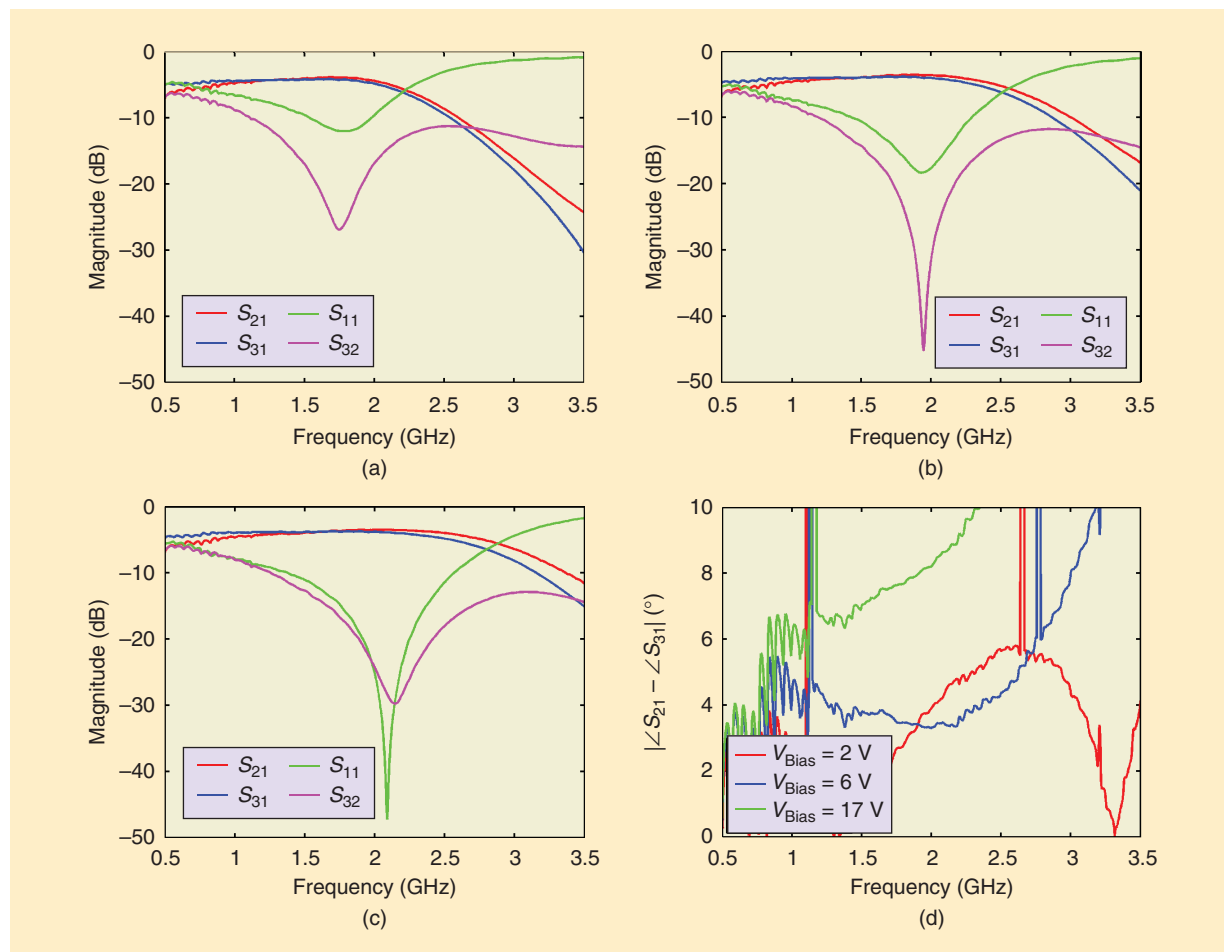


**Figure 9.** Measured  $S$ -parameters of fabricated reduced size frequency agile Wilkinson divider: (a) Bias = 2 V, (b) Bias = 6 V, (c) Bias = 17 V, and (d) Phase relation between output ports.

provide a second degree of freedom for optimum operation at the expense of a second bias voltage.

### Branch-Line Coupler

A tunable branch-line coupler based on our design methodology was fabricated on Rogers RO3010 substrate and is shown in Figure 8(b). The targeted operating frequency range is again 1.7–2.4 GHz for covering all relevant communication bands. Ideally, the coupler should achieve equal 3 dB power splitting and 90° phase shift between its outputs while preserving sufficient isolation between them at all operating states. There are dc-block capacitors placed at all RF ports, and one RF choke inductor is employed to isolate the tuning voltage used to establish the proper bias conditions for the ferroelectric tuning varactors. Varactors with a nominal maximum capacitance of 3 pF serve as tuning elements. Given the moderate varactor quality factors and their tunability, the coupler frequency varied from 1.8 GHz to 2.3 GHz, achieving a tunability range of 27%. The measured insertion loss shown in Figure 11 is compared to the 3 dB coupling and varies from 2 dB to 2.7 dB, depending on the applied bias state. The worst-case deviation from the nomi-

nal phase difference of 90° is  $\pm 5^\circ$ . Similar differences are observed for the amplitude, where the maximum difference for each bias state is 0.4 dB. The achieved attenuation for the second harmonic exceeds 30 dB at all operating conditions.

## Reconfigurable Microwave Circuits

### LC Coupler

Based on the analysis introduced in the “Quadrature Couplers” section, a tunable LC-coupler has been implemented in [16]. Figure 12 shows a block diagram of the coupler, which consists of a variable capacitor and a variable inductor. Two eigenreflections are fixed at  $-1$  and  $1$ . The other two eigenreflections can be adjusted independently by tuning either the capacitor or the inductor. Therefore, the coupler works at arbitrary frequencies with arbitrary coupling ratios and, ideally, the circuit is perfectly matched and isolated at all frequencies. However, at microwave frequencies, tunable inductors are difficult to fabricate and yield poor port balance. A possible realization is shown in Figure 12. The structure consists of two 50  $\Omega$  microstrip lines that are connected by a variable capacitance

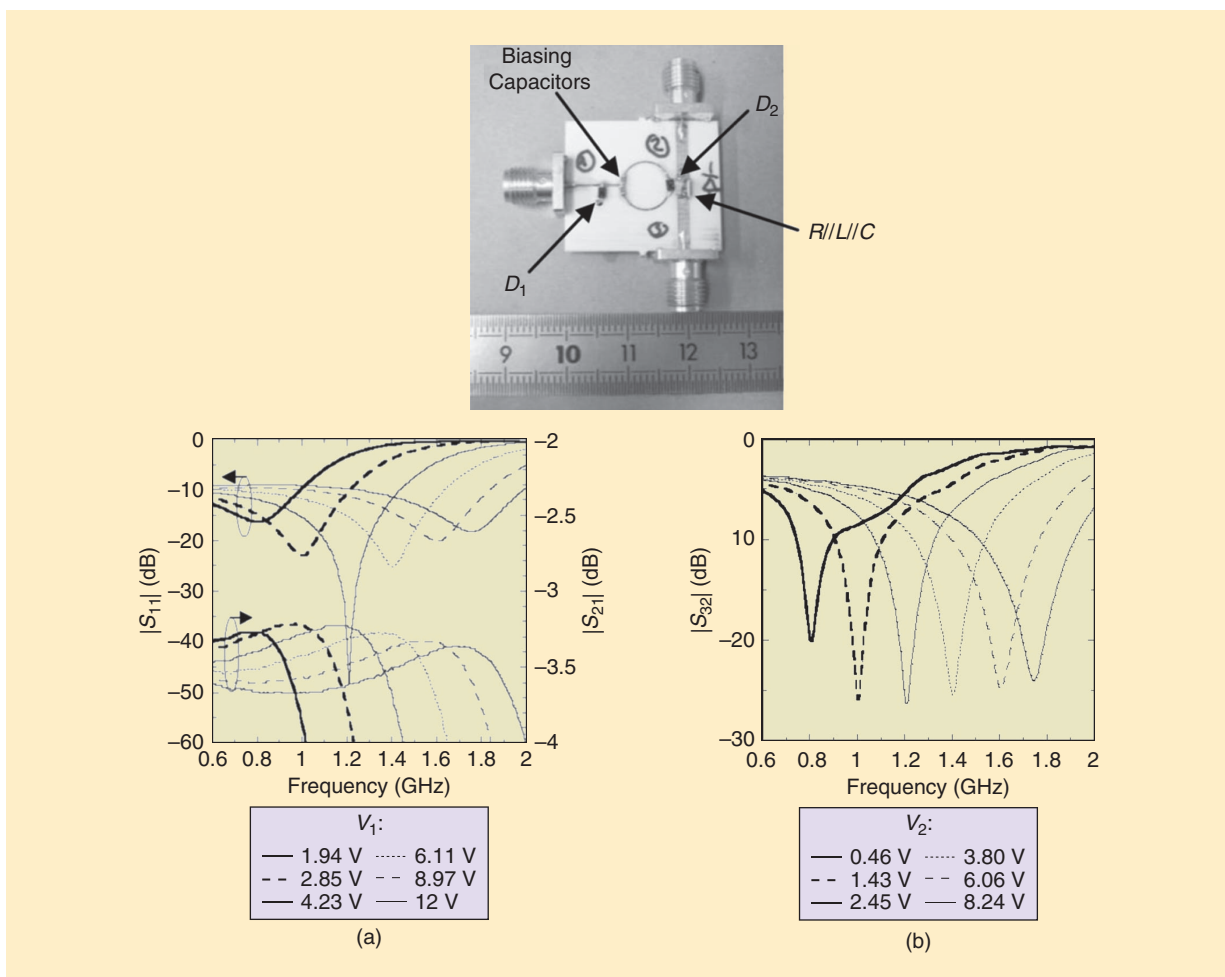
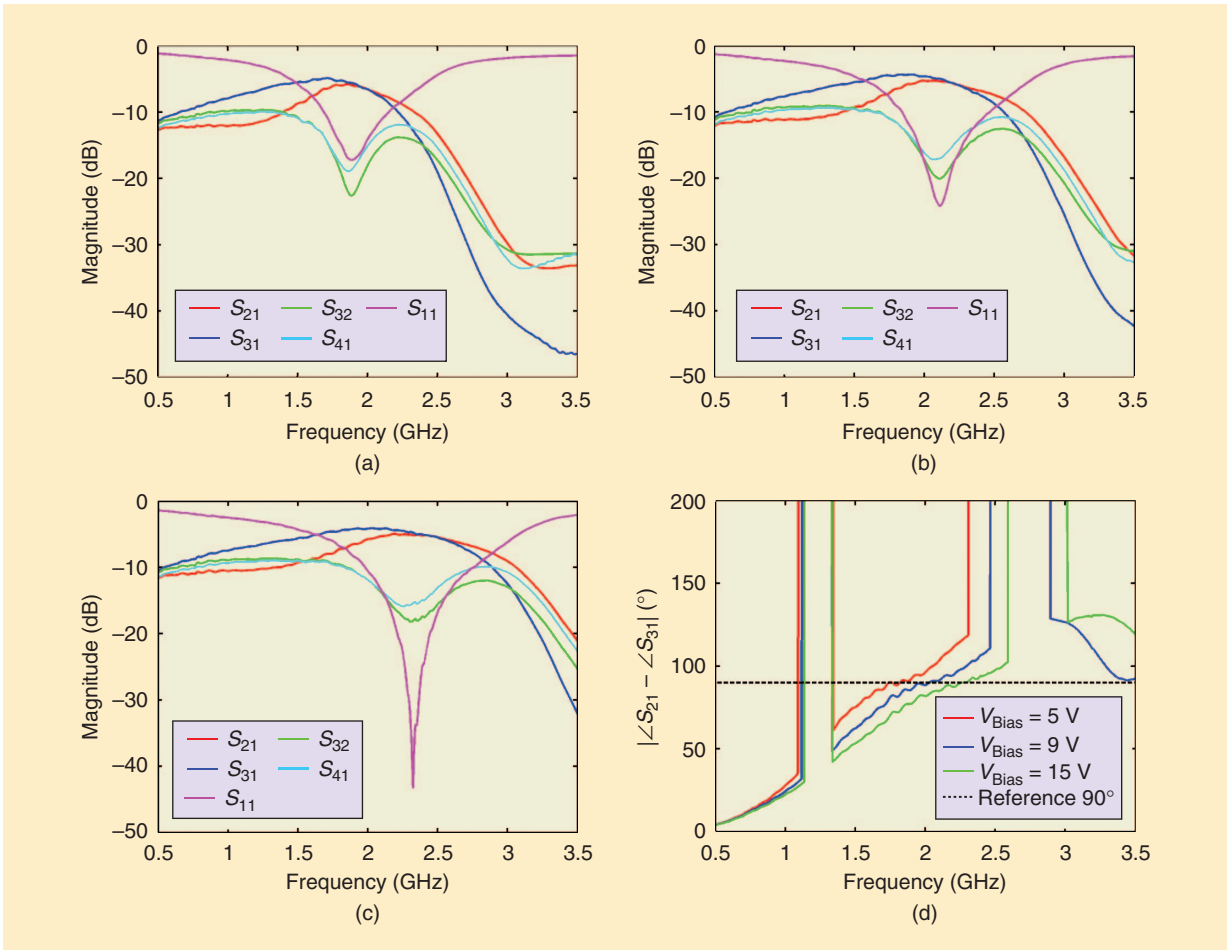


Figure 10. Prototype circuit and experimental results of tunable power divider (data from [25]).

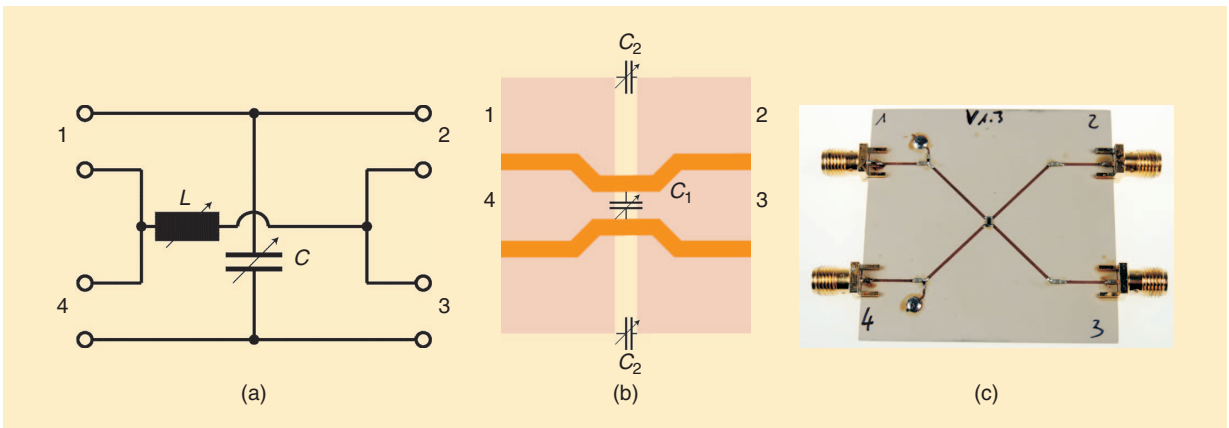


**Figure 11.** Measured  $S$ -parameters of fabricated reduced size frequency agile branch-line coupler: (a) Bias = 5 V, (b) Bias = 9 V, (c) Bias = 15 V, and (d) phase relation between output ports.

on the top layer. A slot line loaded with two variable capacitances is defined in the ground plane. A transformation through the slot line leads to a virtual variable inductance in between the middle of the slot line. The coupler theoretically works at arbitrary frequencies with an arbitrary coupling ratio, however, matching and directivity are no longer frequency independent. In the practical circuit, the variable capacitors are real-

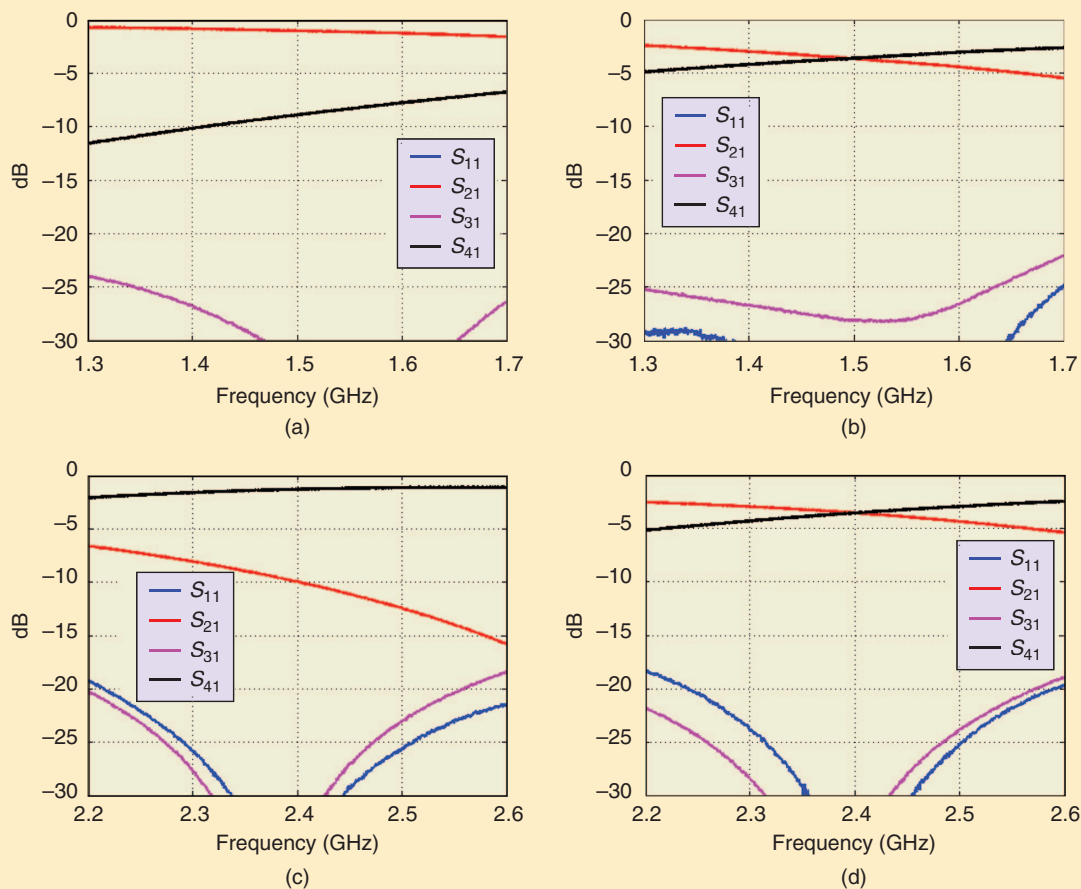
ized by varactor diodes. On the top layer, dc bias for the diode is supplied via high value resistors.

Figure 13 shows the measured results. The coupler's operating frequency can be shifted continuously from 1.5 GHz to 2.4 GHz, achieving a tunability range of 60%. At 1.5 GHz, the coupling to port 4 can be adjusted from  $-8.9$  dB to  $-3.6$  dB while the coupler loss increases from 0.36 dB to 0.65 dB. At 2.4 GHz, the tuning range is



**Figure 12.** LC coupler, principal circuit, and realization at microwave frequencies.





**Figure 13.** LC coupler, measurement results, variation of coupling ratio, and operating frequency: (a)  $Bias_{D1} = 30$  V and  $Bias_{D2} = 10.3$  V, (b)  $Bias_{D1} = 14.7$  V and  $Bias_{D2} = 3.2$  V, (c)  $Bias_{D1} = 10.5$  V and  $Bias_{D2} = 15.6$  V, and (d)  $Bias_{D1} = 20.8$  V and  $Bias_{D2} = 28$  V.

from  $-3.6$  dB to  $-1.3$  dB while the loss is from  $0.55$  dB to  $0.75$  dB. Reconfigurable couplers with variable coupling ratios can be used in combination with power amplifiers to achieve improved efficiency at a certain operating frequency. As demonstrated in [33], where the LC coupler of Figure 12 is used, controlling the amount of coupling in a sequential amplifier results in improved efficiency under back-off operation, which is essential for a transmitter module.

### Cascaded Couplers

The cascading of directional couplers and insertion of discontinuities in the connection branches offers countless possibilities for the development of couplers having tunable coupling ratios. Here, a cascade of two 3 dB forward couplers using variable capacitors in the connection branches, which are shorted to ground, is presented. Figure 14 shows the circuit schematic and the fabricated prototype. The prototype consists of a capacitor, an inductor, two  $50\ \Omega$  transmission lines, and two variable capacitors shorted to ground [24]. It should be noted that there is ideally no proximity coupling between the transmission lines. The entire structure realizes a tunable  $0^\circ/180^\circ$  backward coupler. The

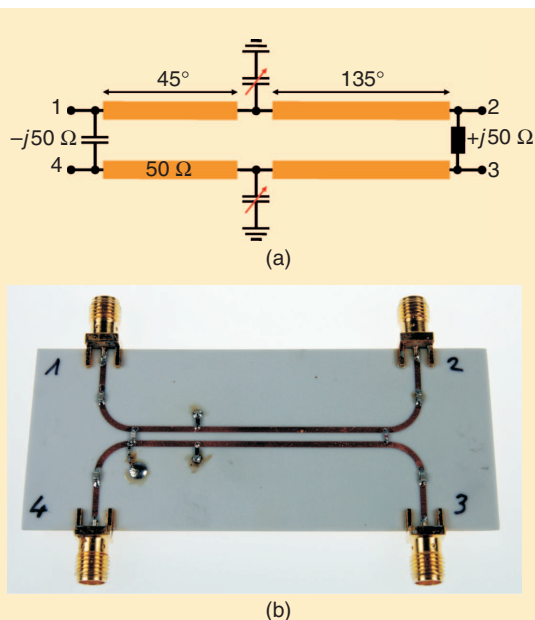


**Figure 14.** Coupler with tunable coupling ratios by cascading two forward couplers and insertion of discontinuities.

## Well-known microwave circuits such as power dividers and couplers can be made extremely versatile by the introduction of tunable passive components.

dc bias for the varactors is supplied via a high-value resistor.

In Figure 15, the measured scattering parameters of three coupling configurations of the prototype are depicted for the excitation of port 1. The center frequency is 1.93 GHz. The coupling to port 4 can be tuned from  $-13.2$  dB to  $-0.94$  dB, while the transmission coefficient

TABLE 1. Comparison of tunable and reconfigurable coupler/divider circuits.

Reference	Topology	Type	Tuning Element	Frequency	Coupler/Divider Ratio
[25]	Divider	Semilumped	Varactor Diode	0.9–1.7 GHz	3 dB
[27]	Divider	Semilumped	MEMS switch	12 GHz	3–25 dB
[14] and this work	Divider	Semilumped	Ferroelectric Varactor	1.7–2.1 GHz	3 dB
[15]	Coupler	Lumped	Ferroelectric Varactor	1.7–2.1 GHz	3 dB
[26]	Coupler	Semilumped	Varactor Diode	1.5–7 GHz	3 dB
[28]	Coupler	Semilumped	MEMS switch	18 GHz	10–17 dB
[29]	Coupler	Semilumped	Varactor Diode	1.5 GHz	6–10 dB
[30]	Coupler	Lumped Active	MOS Varactor	2.1–3.1 GHz	1.4–7.1 dB
[14] this work	Coupler	Semilumped	Ferroelectric Varactor	1.8–2.3 GHz	3 dB
[16] this work	Coupler	Semilumped	Varactor Diode	1.5–2.4 GHz	1.3–8.9 dB
[24] this work	Coupler	Semilumped	Varactor Diode	1.9 GHz	0.9–13.2 dB

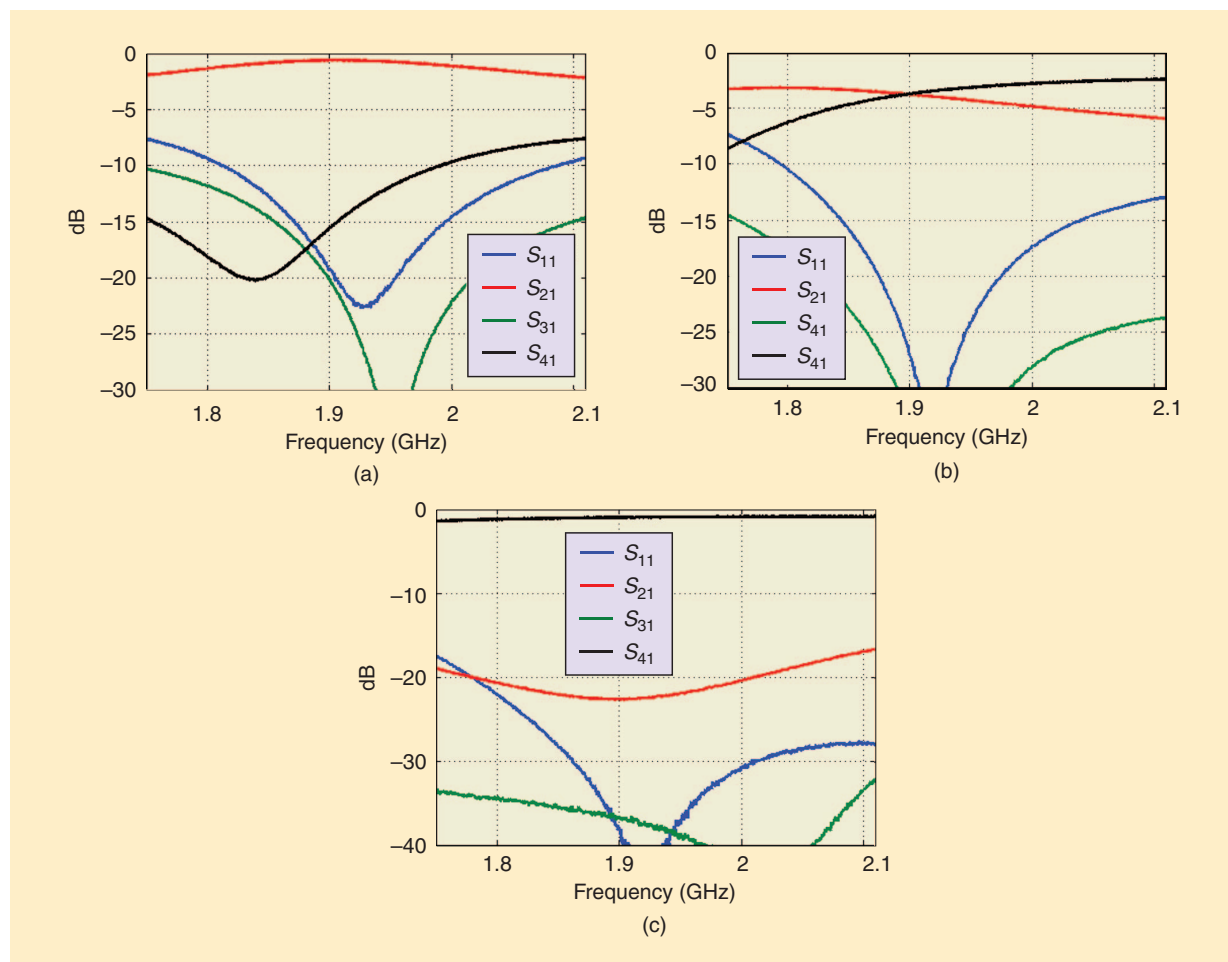


Figure 15. Measurement results: (a) bias = 30 V, (b) bias = 11.6 V, and (c) bias = 4.8 V.

between port 1 and port 2 varies from  $-0.65$  dB to  $-22.4$  dB. The coupler loss is between 0.4 dB to 0.9 dB.

In order to provide a comparison of the circuit characteristics presented in this article with other investigators work, a number of reconfigurable and tunable coupler/divider circuit examples are summarized in Table 1.

## Conclusion

As demonstrated with various implementations in this article, well-known microwave circuits such as power dividers and couplers can be made extremely versatile by the introduction of tunable passive components. Analytical design methodologies have been discussed, which enable frequency agile and reconfigurable characteristics for the investigated coupler/divider topologies. Depending on the target application, the coupler/divider circuits can be tuned for different frequencies and coupling ratios and combined with active circuitry such as power amplifiers. The resulting reconfigurable functional blocks can finally operate in complex RF transceiver architectures and pave the way to multiband and multimode operation for future communication devices.

## References

- [1] C. Hoarau, N. Corrao, J. D. Arnould, P. Ferrari, and P. Xavier, "Complete design and measurement methodology for a tunable RF impedance-matching network," *IEEE Trans. Microwave Theory Tech.*, vol. 56, no. 11, pp. 2620–2627, Nov. 2008.
- [2] M. Schmidt, E. Lourandakis, A. Leidl, S. Seitz, and R. Weigel, "A comparison of tunable ferroelectric  $\Pi$ - and  $T$ -matching networks," in *Proc. 37th European Microwave Conf.*, Oct. 9–12, 2007, pp. 98–101.
- [3] M. Nguyen, W. Yan, and E. Horne, "Broadband tunable filters using high Q passive tunable ICs," in *IEEE MTT-S Int. Microwave Symp. Dig.*, June 15–20, 2008, pp. 951–954.
- [4] E. Lourandakis, M. Schmidt, G. Fischer, and R. Weigel, "A ferroelectric tunable combline filter with improved stopband transitions," in *Proc. IEEE Radio and Wireless Symp.*, Jan. 18–22, 2009, pp. 340–343.
- [5] F. Ali, E. Lourandakis, R. Gloeckler, K. Abt, G. Fischer, and R. Weigel, "Tunable multiband power amplifier using thin-film BST varactors for 4G handheld applications," in *Proc. IEEE Radio and Wireless Symp.*, Jan. 2010, pp. 236–239.
- [6] J.-S. Fu and A. Mortazawi, "Improving power amplifier efficiency and linearity using a dynamically controlled tunable matching network," *IEEE Trans. Microwave Theory Tech.*, vol. 56, no. 12, pt. 2, pp. 3239–3244, Dec. 2008.
- [7] S. Gevorgian, "Agile microwave devices," *IEEE Microwave Mag.*, vol. 10, no. 5, pp. 93–98, Aug. 2009.
- [8] A. Koelpin, G. Vinci, B. Laemmle, D. Kissinger, and R. Weigel, "The six-port in modern society," *IEEE Microwave Mag.*, vol. 11, no. 7, pp. 35–43, Dec. 2010.
- [9] E. E. Djoumessi, S. O. Tatu, R. G. Bosisio, M. Chaker, and K. Wu, "Varactor-tuned multi-band six-port front-end for wireless applications," in *Proc. Asia-Pacific Microwave Conf.*, Dec. 16–20, 2008, pp. 1–5.
- [10] S. Y. Zheng, S. H. Yeung, W. S. Chan, K. F. Man, and S. H. Leung, "Size-reduced rectangular patch hybrid coupler using patterned ground plane," *IEEE Trans. Microwave Theory Tech.*, vol. 57, no. 1, pp. 180–188, Jan. 2009.
- [11] K. S. Chin, K. M. Lin, Y. H. Wei, T. H. Tseng, and Y. J. Yang, "Compact dual-band branch-line and rat-race couplers with stepped-impedance-stub lines," *IEEE Trans. Microwave Theory Tech.*, vol. 58, no. 5, pp. 1213–1221, May 2010.
- [12] I.-H. Lin, C. Caloz, and T. Itoh, "A branch-line coupler with two arbitrary operating frequencies using left-handed transmission lines," in *IEEE MTT-S Int. Microwave Symp. Dig.*, June 8–13, 2003, pp. 325–328.
- [13] T. Hirota, A. Minakawa, and M. Muraguchi, "Reduced-size branch-line and rat-race hybrids for uniplanar MMICs," *IEEE Trans. Microwave Theory Tech.*, vol. 38, no. 3, pp. 270–275, Mar. 1990.
- [14] E. Lourandakis, M. Schmidt, S. Seitz, and R. Weigel, "Reduced size frequency agile microwave circuits using ferroelectric thin-film varactors," *IEEE Trans. Microwave Theory Tech.*, vol. 56, no. 12, pt. 2, pp. 3093–3099, Dec. 2008.
- [15] E. A. Fardin, A. S. Holland, and K. Ghorbani, "Frequency agile 90 deg hybrid coupler using barium strontium titanate varactors," in *IEEE MTT-S Int. Microwave Symp. Dig.*, June 3–8, 2007, pp. 675–678.
- [16] H. Mextorf, T. Lehmann, and R. Knoechel, "Systematic design of reconfigurable quadrature directional couplers," in *IEEE MTT-S Int. Microwave Symp. Dig.*, 2009, pp. 1009–1012.
- [17] J. Reed and G. J. Wheeler, "A method of analysis of symmetrical four port networks," *IRE Trans. Microwave Theory Tech.*, vol. 4, no. 4, pp. 246–252, 1956.
- [18] T. Lehmann, H. Mextorf, and R. Knoechel, "Design of quadrature directional couplers with continuously variable coupling ratios," in *Proc. 38th European Microwave Conf.*, 2008, pp. 199–202.
- [19] K. R. Bushore and W. L. Teeter, "A variable-ratio microwave power divider and multiplexer," *IRE Trans. Microwave Theory Tech.*, vol. 5, no. 4, pp. 227–229, 1957.
- [20] A. Ocera, R. V. Gatti, P. Farinelli, and R. Sorrentino, "A MEMS programmable power divider/combiner for reconfigurable antenna systems," in *Proc. European Microwave Conf.*, 2005, vol. 1, pp. 621–624.
- [21] L. Nyström, "A new microwave variable power divider," *IEEE Trans. Microwave Theory Tech.*, vol. 27, no. 1, pp. 89–90, 1979.
- [22] M. S. Navarro, S. N. Prasad, M. Abderson, and D. Gardner, "Non-reflecting electronically variable attenuator," in *Proc. Microwave and Optoelectronics Conf.*, 1999, vol. 2, pp. 541–544.
- [23] R. V. Gatti, A. Ocera, S. Bastioli, L. Marcaccioli, and R. Sorrentino, "A novel compact dual band reconfigurable power divider for smart antenna systems," in *IEEE MTT-S Int. Microwave Symp. Dig.*, 2007, pp. 423–426.
- [24] H. Mextorf, T. Lehmann, and R. Knoechel, "Compact cascaded directional couplers with continuously tuneable coupling ratios," in *Proc. German Microwave Conf.*, 14–16 March 2011, pp. 1–4.
- [25] A.-L. Perrier, O. Exshaw, J.-M. Duchamp, and P. Ferrari, "A semi-lumped miniaturized spurious less frequency tunable three-port divider combiner with 20 dB isolation between output ports," in *IEEE MTT-S Int. Microwave Symp. Dig.*, 2006, pp. 1714–1717.
- [26] F. Ferrero, C. Luxey, R. Staraj, G. Jacquemod, and V. F. Fusco, "Compact quasi-lumped hybrid coupler tunable over large frequency band," *Electron. Lett.*, vol. 43, no. 19, pp. 1030–1031, Sept. 2007.
- [27] A. Ocera, P. Farinelli, F. Cherubini, P. Mezzanotte, R. Sorrentino, B. Margesin, and F. Giacomozzi, "A MEMS-reconfigurable power divider on high resistivity silicon substrate," in *IEEE MTT-S Int. Microwave Symp. Dig.*, 2007, pp. 501–504.
- [28] L. Marcaccioli, P. Farinelli, M. M. Tentzeris, J. Papapolymerou, and R. Sorrentino, "Design of a broadband MEMS-based reconfigurable coupler in Ku-band," in *Proc. 38th European Microwave Conf.*, 2008, pp. 595–598.
- [29] S.-M. Wang, C.-Y. Chang, and J. Lin, "A software configurable coupler with programmable coupling coefficient," in *IEEE MTT-S Int. Microwave Symp. Dig.*, 2007, pp. 185–188.
- [30] M. A. Y. Abdalla, P. Khoman, and G. V. Eleftheriades, "A compact highly reconfigurable CMOS MMIC directional coupler," *IEEE Trans. Microwave Theory Tech.*, vol. 56, no. 2, pp. 305–319, Feb. 2008.
- [31] S. Kwon, M. Kim, S. Jung, J. Jeong, K. Lim, J. Van, H. Cho, H. Kim, W. Nah, and Y. Yang, "Inverted-load network for high-power Doherty amplifier," *IEEE Microwave Mag.*, vol. 10, no. 1, pp. 93–98, Feb. 2009.
- [32] J. Lim, C. Park, J. Koo, H. Cha, Y. Jeong, and S. M. Han, "A balanced power amplifier utilizing the reflected input power," in *Proc. IEEE Symp. Radio Frequency Integration Technology*, 2009, pp. 88–91.
- [33] T. Lehmann and R. Knoechel, "Sequential power amplifiers with adaptable combiners," in *IEEE MTT-S Int. Microwave Symp. Dig.*, June 2009, pp. 425–428.

